# Conformational studies and pore-forming properties of an α-amino-isobutyric acid analogue of gramicidin B

**Masood Jelokhani-Niaraki,[a] Hiroaki Kodama,[a] Tsuguhisa Ehara[b] and Michio Kondo*,[a]**
[a] *Department of Chemistry, Faculty of Science and Engineering, Saga University, Honjomachi, Saga 840, Japan*
[b] *Department of Physiology, Saga Medical School, Nabeshima, Saga 849, Japan*

Structure-function relation of a designed α-aminoisobutyric acid (Aib) analogue of gramicidin B (GBA), a model for helical protein structures, is examined by CD and patch-clamp experiments. This 16-residue peptide adopts stable helical structures in organic and aqueous solvent sytems, and phospholipid vesicles. The content of the helical structure in egg yolk phosphatidylcholine vesicles increases with the increase of lipid-to-peptide molar ratio, suggesting adsorption and incorporation processes. A possible helix–helix interaction is observable at low peptide-to-lipid molar ratios. The role of Trp side-chains for the rather high affinity of this peptide for membrane surfaces is stressed. Though shorter than the average thickness of phospholipid bilayers, GBA forms voltage-dependent multi-state ion-conducting pores in diphytanoyl phosphatidylcholine bilayers formed at the tip of micropipettes, at relatively low concentrations. A range of GBA conductances is comparable to membrane protein channels. GBA pores show a variety of conducting behaviours as well as rectifying properties.

Ion channels in cell membranes are typically high molecular weight proteins which are able to interact with membranes through long- and short-range interactions, and have access to both intra- and extra-cellular milieus as well as the membrane intermediate hydrophobic layer and its hydrophilic boundaries. The channel structures might either result from an assembly of several subunits through interaction of the appropriate secondary structures or from an internal repeat of certain structures in a single chain.[1]

The main features of ion channel proteins—such as gating mechanism, ion selectivity, voltage dependence and conductance—can be modelled in the less sophisticated peptide systems. Gramicidin and alamethicin (Fig. 1) are two of such peptides with much smaller molecular weights than the channel proteins, and only one predominant motif in their secondary structures in membranes. Gramicidin is a hydrophobic 16-residue peptide from *Bacillus brevis* which forms a $\beta^{6.3}$-helical head-to-head dimerical channel (*ca.* 0.4 nm in diameter) in phospholipid bilayers showing monovalent cation selectivity, whereas in organic solvents gramicidin adopts a variety of structures different from those in phospholipids.[2,3] On the other hand, alamethicin, an amphipathic 20-residue peptide isolated from the fungus *Trichoderma viride*, is largely α-helical in phospholipid vesicles,[4,5] and in organic solvents,[6] and its pore structure is believed to be comprised of a bundle of helices packed laterally in a direction perpendicular to the membrane plane.[7,8] Alamethicin represents a group of peptide antibiotics termed as peptaibols, all of which have a rather high content of α-aminoisobutyric acid (Aib) (25–50%), and consist of 16–20 amino acids. Peptaibols are believed to form helical structures in phospholipids, and the presence of Aib, with its preference for certain dihedral angles most suitable for $3_{10}$- or α-helical secondary structures,[9] gives a particular stability to their conformations in a variety of environments. Conformational and electrophysiological properties of alamethicin and peptaibols, as well as their analogues and other Aib-containing peptides, have been reviewed in detail.[3,10–13]

Although gramicidin-like structures have not hitherto been found in proteins, gramicidin-like channel functions, such as ion selectivity and subconducting states, are well encountered in channel-forming proteins. On the other hand, $3_{10}$- and α-helices are two of the secondary structures found in proteins,[14] and the proposed helix-bundle structure of alamethicin has much in common with the hypothesized barrel-like structures of channel proteins such as nicotinic acetylcholine receptor (nAChR).[15] The main shortcoming is the very weak ion selectivity,[16] and comparably high conductance levels in alamethicin-like pores.[17,18] Both gramicidin and alamethicin are structurally less stable and less selective in comparison to the channel proteins.

Alamethicin: ($R_f$50) Ac-Aib-L-Pro-Aib-L-Ala-Aib$^5$-L-Ala-L-Gln-Aib-L-Val-Aib$^{10}$-Gly-L-Leu-Aib-L-Pro-L-Val$^{15}$-Aib-Aib-L-Gln-L-Gln-L-Pheol$^{20}$

Gramicidin B: Formyl-L-Val-Gly-L-Ala-D-Leu-L-Ala$^5$-D-Val-L-Val-D-Val-L-Trp-D-Leu$^{10}$-L-Phe-D-Leu-L-Trp-D-Leu-L-Trp$^{15}$-Glyol

GBA: Formyl-L-Val-Gly-L-Ala-Aib-L-Ala$^5$-Aib-L-Val-Aib-L-Trp-Aib$^{10}$-L-Phe-Aib-L-Trp-Aib-L-Trp$^{15}$-Glyol

**Fig. 1** Primary structures of peptides. Ac- stands for the acetyl at the *N*-terminus; Pheol and Glyol are the corresponding amino alcohols of Phe and Gly, respectively, located at the *C*-termini.

In a previous study, in order to mimic the stable helical structures of proteins with pore-forming ability and by considering gramicidin and alamethicin primary structures, we synthesized gramicidin Aib analogues, in which all of the six alternatively placed D-amino acids in the gramicidin backbone were replaced with Aibs.[19] Circular dichroic (CD) comparative studies of these analogues and gramicidin showed basically different helical structures in a variety of organic solvents. A rather stable, predominantly α-helical, structure was attributed to the analogues, and the drastic reduction in their antimicrobial activities against certain gram-positive bacteria, in comparison with gramicidin, was supposed to be a result of structural differences. Indeed, the structural difference in phospholipid bilayers was observed in a later comparative study.[20]

In the present study, we further discuss the structural characteristics of a representative gramicidin B Aib analogue (GBA) (Fig. 1) in solution and phospholipid vesicles. Electrophysiological measurements in phospholipid bilayers implies the pore-forming ability of this analogue. The functional characteristics of GBA in membranes show a range of

**Table 1** Circular dichroic characteristics of GBA

| Solvent (% v/v) | | Maximum wavelength/nm ([θ]) | Minimum wavelength(s)[a]/nm ([θ]) | $[\theta]_{222}$ | $[\theta]_{233}/[\theta]_{222}/[\theta]_{216}/[\theta]_{209}$ |
|---|---|---|---|---|---|
| Ethanol–water | (100) | 193.0 (43 360) | 209.0 (−20 330), 216.2 (−19 180), 233.2 (−8 267) | −16 070 | 0.41/0.79/0.94/1.00 |
| | (75) | 193.2 (38 020) | 209.0 (−18 600), 216.4 (−17 660), 232.6 (−8 379) | −14 870 | 0.45/0.80/0.95/1.00 |
| | (50) | 193.6 (34 690) | 209.0 (−15 540), 216.4 (−15 250), 233.0 (−7 498) | −13 140 | 0.48/0.84/0.98/1.00 |
| | (25) | 195.6 (28 000) | *211.4* (−12 430), 218.0 (−12 800), *233.0* (−8 545) | −12 530 | 0.76/1.12/1.13/1.00 |
| | (4) | 195.4 (27 280) | *211.4* (−10 040), 219.4 (−11 230), *233.0* (−6 591) | −11 020 | 0.72/1.21/1.17/1.00 |
| Methanol–water | (100) | 192.4 (40 320) | 209.0 (−19 260), 215.8 (−18 280), 232.4 (−8 822) | −14 680 | 0.45/0.76/0.95/1.00 |
| | (75) | 193.4 (33 860) | 209.0 (−15 570), 215.6 (−15 260), 230.8 (−8 187) | −12 610 | 0.50/0.81/0.98/1.00 |
| | (50) | 193.6 (27 070) | *212.0* (−10 210), 217.8 (−11 500), *230.8* (−7 256) | −10 180 | 0.73/1.06/1.17/1.00 |
| | (25) | 196.4 (23 900) | *212.0* (−8 451), 219.6 (−9 877), *233.0* (−6 751) | −9 703 | 0.95/1.37/1.30/1.00 |
| | (1) | 195.4 (19 140) | *211.2* (−7 463), 220.2 (−8 030), *234.0* (−5 159) | −7 972 | 0.77/1.13/1.09/1.00 |
| Octan-1-ol–TFE | (100) | 194.2 (39 810) | 209.6 (−15 810), 217.0 (−15 520), 234.0 (−6 067) | −14 130 | 0.38/0.90/0.98/1.00 |
| | (96) | 192.6 (37 990) | 209.6 (−15 900), 215.4 (−15 540), 234.4 (−5 965) | −13 390 | 0.36/0.84/0.98/1.00 |
| | (75) | 193.0 (33 540) | 209.4 (−15 290), 215.4 (−15 070), 233.6 (−6 551) | −10 400 | 0.42/0.75/0.99/1.00 |
| | (50) | 192.6 (27 530) | 209.4 (−14 230), *215.6* (−13 730), 232.8 (−5 771) | −8 742 | 0.40/0.61/0.96/1.00 |
| | (25) | 193.0 (24 710) | 210.6 (−14 060), 213.8 (−14 130), 231.6 (−5 861) | −7 691 | 0.40/0.55/0.97/1.00 |
| TFE | (100) | 193.0 (22 480) | *209.0* (−12 400), 213.2 (−12 190), 231.2 (−5 394) | −5 802 | 0.41/0.47/0.96/1.00 |
| Dioxane | (100) | — | 209.2 (−22 300), 217.8 (−20 510), *232.2* (−10 220) | −19 000 | 0.45/0.85/0.91/1.00 |
| EYPC in water (PL 1:50) | (pH 6–7) | 194.0 (28 530) | 210.2 (−9 691), 220.6 (−10 520), *234.0* (−6 409) | −10 450 | 0.72/1.10/1.03/1.00 |
| EYPC in water (PL 1:100) | (pH 6–7) | 194.6 (34 760) | 210.4 (−14 130), 221.2 (−15 000), *234.0* (−7 928) | −14 900 | 0.61/1.07/1.01/1.00 |

[a] Values in italic are approximate turning points of shoulder-like motifs.

conductances reminiscent of conductance sublevels in channel proteins. An attempt to correlate the CD spectra and electrophysiological data, to interpret the structure–functional relation of this analogue, forms the main body of this report.

## Results and discussion

### CD conformational analysis

A more detailed CD structural analysis of GBA, reveals certain structural characteristics in different solvent systems and egg yolk phosphatidylcholine (EYPC) vesicles. This is shown in some detail in Table 1, where certain characteristic features of the CD spectra such as maxima, minima, and relative mean residue ellipticity values are emphasized. The latter relative values are indicators of certain structural groups and we shall use these values in discussing the structural changes of GBA in different environments.

Figs. 2(*a*) and (*b*) illustrate the conformational changes of GBA and alamethicin in aqueous–alcoholic solvent mixtures, respectively. Alamethicin experiences a regular decrease in its helical structure with increase of the water ratio in a methanol–water solvent system, while preserving its main structural characteristics, *i.e.* showing an isodichroic point at around 201.5 nm, and α-helical distinctive maximum at 193 nm and minima at 209 and 222 nm. On the other hand, GBA shows a characteristic structural change at higher water ratios in aqueous–alcoholic solvents. Both the isodichroic and the maximum points are about 2.5 nm red-shifted, while the regular minima pattern at 209, 216 and 233 nm in more alcoholic solvents is also changed to give rise to a single minimum in the 218–220 nm range in more aqueous solvents. This alcohol-dominant-to-water-dominant structural change can be also followed by considering the relative ellipticities in Table 1. In the ethanol–water solvent mixtures, the alcohol-dominant structure is almost preserved in 100, 75 and 50% ethanol, whereas the relative values for 216, 222 and 233 nm increase and switch to values more than one for 216 and 222 nm in the water-dominant solvents.

Another major difference between the solvent-dependent behaviour of alamethicin and GBA is shown in Fig. 3. In Fig. 3(*a*) the alamethicin CD spectrum in ethanol manifests the main traits of an α-helical conformation, while these traits are not as conventional in the GBA spectrum. Fig. 3(*b*) shows the structures of alamethicin and GBA in dioxane. The content of the helical structure of alamethicin drastically decreases in dioxane, as was previously shown by both CD,[6] and dipole moment studies.[21,22] On the contrary, GBA helical structure in dioxane seems quite predominant with comparable helical contents and spectral patterns to the structures in alcoholic solvents (Table 1). Interestingly a minimum Cotton effect at around 230 nm was also observed in the CD spectra of gramicidin in methanol (though much less intense) and dioxane, and this minimum was also deepened in the latter solvent.[19,23] The similarity of the CD pattern of GBA in dioxane and alcohols at relatively low concentrations (the spectra in alcoholic solvents did not show a considerable change in concentration ranges between 10 to 600 μmol $dm^{-3}$), mentioned above, can suggest the presence of a predominantly monomeric state in these milieus.

Structural features of GBA were also studied in non-aqueous solvent systems such as octan-1-ol–trifluoroethanol (TFE). Octan-1-ol is a hydrophobic alcohol with a low relative permittivity (10.34), and dipole moments comparable to water or ethanol (1.76 D). The long hydrocarbon chain of this alcohol, carrying a polar function, implies similiarities with the phospholipid bilayer amphipathic environments. The solvent-dependent attitude of GBA is shown in Table 1. GBA adopts its typical alcoholic structure in octan-1-ol, and the addition of TFE causes a decrease in the helical content of the peptide as have been observed for alamethicin in the same set of solvents (unpublished results).

In these comparative studies, the rigidity of GBA helical structure (and also its relative helix content) seems to be more pronounced than alamethicin under the same conditions. The general pattern of GBA spectra has not been observed for the other synthetic periodically sequenced Aib peptides,[24,25] or peptaibols.[6,26] The distortion in spectra might be caused by Trp interaction. The interaction of Trp residues with CD spectra of peptides, such as gramicidin, and proteins has been emphasized.[27,28]

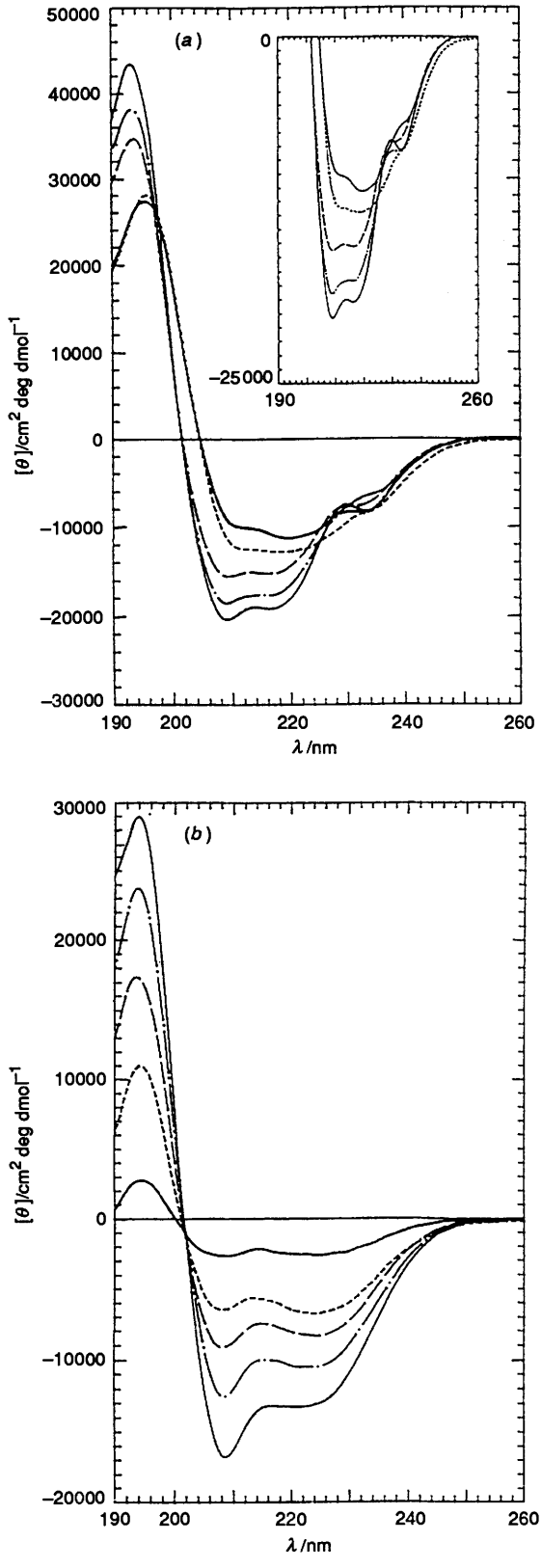


**Fig. 2** CD spectra of (*a*) GBA in the ethanol–water solvent system: 100% (—— bottom), 75% (— · —), 50% (— — —). 25% (- - - -) and 4% (—— top); and (*b*) alamethicin in the methanol–water solvent system: 100%(——bottom), 75%(— · —), 50%(— — —), 25%(- - - -), water (—— top). Percentage values are corresponding to the alcohol content by volume; the order of the above mentioned spectra is considered in the negative ellipticity area, and this order is reversed in the positive ellipticity area; peptide concentrations were 40 μmol $dm^{-3}$ for GBA and 41 μmol $dm^{-3}$ for alamethicin; the room temperature was 22 ± 1 °C.

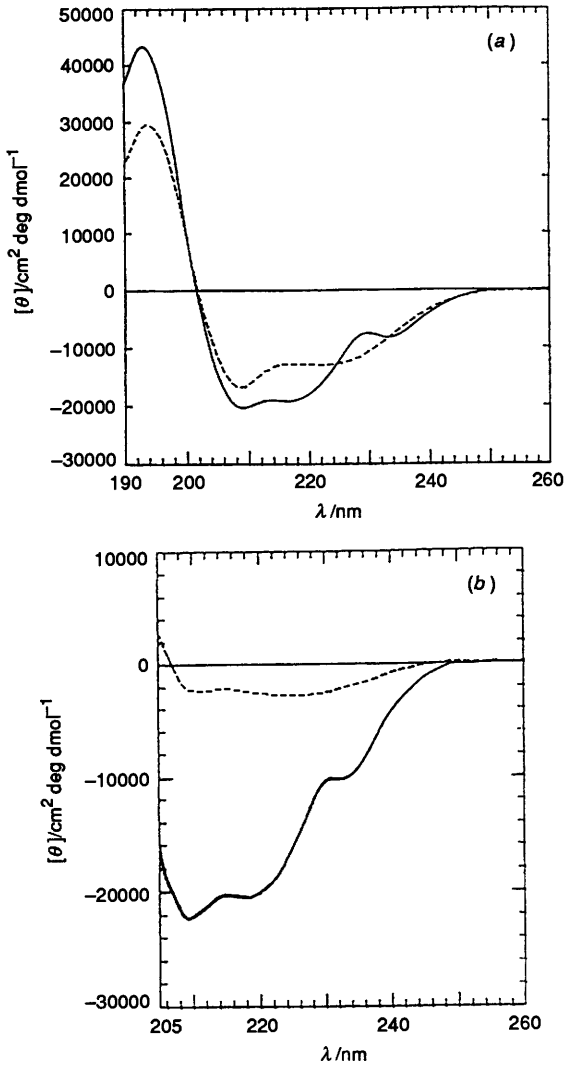


**Fig. 3** Comparison of the CD spectra of GBA (——) and alamethicin (- - - -) in (*a*) ethanol and (*b*) dioxane. Peptide concentrations were 41 μmol $dm^{-3}$ in ethanol and 40 μmol $dm^{-3}$ in dioxane; the room temperature was 22 ± 1 °C

An interesting result was observed in the CD spectra of GBA in phospholipid vesicles, shown in Fig. 4. A comparison between the CD spectra of gramicidin, alamethicin and GBA in aqueous and dipalmitoyl phosphatidylcholine (DPPC) vesicles, at higher peptide-to-lipid ratios, was reported previously.[20] Fig. 4(*a*) shows the changes in GBA structure when transferred from an aqueous solution to phospholipid vesicles. Certain similarities between the three spectra are observable both in the location of their negative Cotton effect minima and relative ellipticities (Table 1). CD spectrum of GBA, in peptide-to-lipid molar ratio of 1:100 (PL 1:100), shows an almost classical helical pattern.

From the data presented in Fig. 4, it becomes apparent that GBA interacts with phospholipid membranes in a concentration-dependent manner, and the CD spectra in the latter environments are more similar to the CD traits in aqueous than organic milieus. This interaction with vesicles (or membranes) is a prerequisite for the pore-forming structures.

### Electrophysiological functions

GBA forms pore-like structures in phospholipid bilayers constituted on glass pipette tips. The conductance of GBA pores has an obvious resemblance to the multi-state conducting behaviour of alamethicin and its related peptides,[12,13] which implies possible structural similarities. Alamethicin can act as

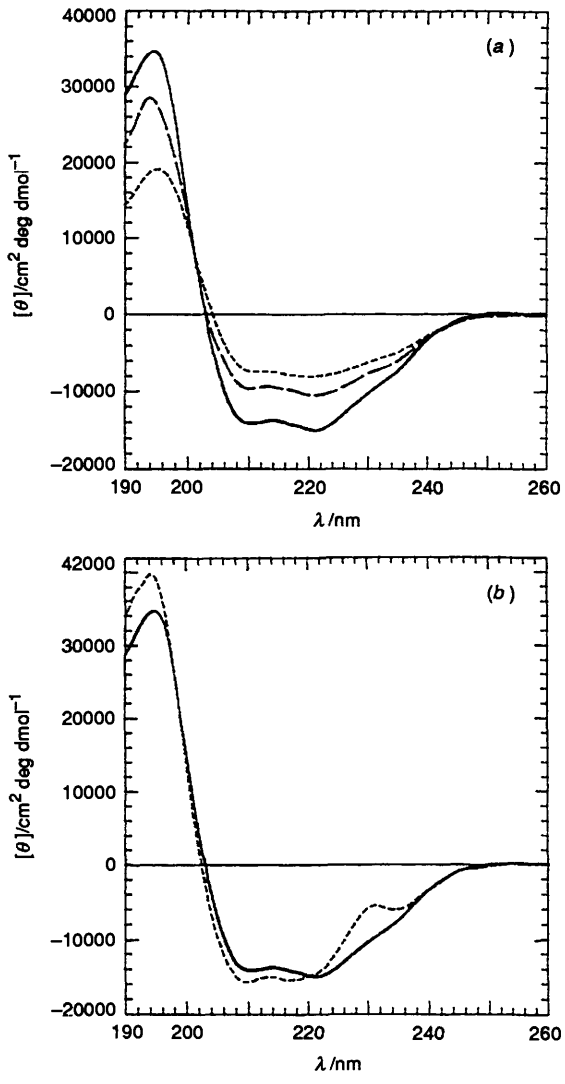


**Fig. 4** (*a*) CD spectra of GBA in water (1% by volume methanol) (– – – –), EYPC vesicles PL 1:50 (— — —) and EYPC vesicles PL 1:100 (——); (*b*) comparison between the CD spectra of GBA in EYPC PL 1:100 (——) and octan-1-ol (– – – –). Peptide concentrations were 10 μmol $dm^{-3}$ in water and EYPC vesicles and 25 μmol $dm^{-3}$ in octan-1-ol; the room temperature was 22 ± 2 °C.

an excitable element in membranes,[29] and forms voltage-gated multi-conductance pore structures in natural[30] and reconstituted lipid bilayers.[31]

Figs. 5 and 6 represent the conductance patterns of GBA pores in diphytanoyl phosphatidylcholine (DPhPC) bilayers at various transmembrane potentials. In Fig. 5(*a*), at 80 mV transmembrane potential, two distinct conductance levels are resolved in the current amplitude histogram. A closer examination of the open-close pattern of the channels reveals certain unresolved sublevels. Generally, the GBA pore in this measurement had a high open probability (more than 0.9). The open state oscillated between certain sublevels and spent most of the time at the higher conductance states (*i.e.* 5th and 6th levels with 39 and 44 pS respective conductances). After a certain period of multi-conductance attitude, the channel spent most of its open time oscillating between levels 2 and 5 [Fig. 5(*a*), lower pattern].

Fig. 5(*b*) illustrates the conductance of the same patch at 100 mV, after an instant decrease of the potential difference to 0 mV and a gradual increase (2–3 mV $s^{-1}$) to 100 mV (the same procedure was repeated twice). This was a shake up to disrupt the stable pore structure. Interestingly, the pore was formed again and its regular conducting patterns were observed within one minute after keeping the potential at 100 mV, though the seal resistance was decreased. This time, higher conductance levels were observed, and apparently the number of sublevels increased. The current amplitude histogram is a rather rough representation of the conductance pattern, but it gives certain resolved conductances at 225 (10), 175 (8), 125 (6), 90 (4) and 50 (2) pS (the number in parenthesis represents the corresponding conductance levels), which might be attributed to groups of close conducting levels. Other conductances are observable in between. The average conductance is best represented by level 6 (*i.e.* 125 pS). The pore spent most of its open state at this level, and the highest and lowest conductance levels had low probabilities. Appearance of higher conductance levels and the change in conductance traits implies the appearance of new pore forms. The higher conductance levels suggest larger pore sizes which can be provided either by a basic overall conformational change, or by the addition of at least one peptide monomer subunit to the barrel-like pore structure. Both of these interpretations have been suggested to account for the behaviour of alamethicin-like pores.[8,32]

At certain points, like the case shown in Fig. 5(*b*), almost all of the conductance levels appear in a burst (a considerably fast open-close mechanism), and then the channel conductance switches to the more stable structures with frequent oscillation between a few intermediate levels.

Other varieties of the pore-forming behaviour of GBA, at a lower ionic strength (0.15 mol $dm^{-3}$ KCl), are shown in Fig. 6. Fig. 6(*a*) shows a predominant single-state conductance, at 80 mV, with very short life-times (closed probability *ca.* 0.9) and high conductances (687.5 pS), which implies an unstable open state, but a permanent pore structure. The same patch in a previous conductance pattern, at the same transmembrane potential, showed an overall oscillation between certain levels with respective conductances at 137.5 and 269 pS (data not shown). The transmembrane potential in Fig. 6(*a*) was reversed instantaneously to −80 mV, and resulted in much lower conductances (*ca.* 60–120 pS) [Fig. 6(*b*)]. Fig. 6(*c*) shows the GBA conductance pattern at transmembrane potential of −190 mV. The main conductance levels have approximate values of 16 and 90 pS, which represent at least two distinct conducting states.

A simple estimation of the pore size of a bundle of rigid cylinders (in our case helices), by taking into account both the Ohmic pore resistance and the access resistance for both sides of the pore, was proposed before.[33] In these calculations, the addition or deletion of a single helical cylinder causes a respective increase or decrease in the conductance of the pore.

The model, mentioned above, was used to estimate the pore sizes and the number of helices (N) of GBA oligomers at two different salt concentrations (Table 2). The helix parameters are the same as those used for alamethicin and zervamicin.[12] Theoretical conductances are in a reasonable agreement with the main experimental conductances. Most of the calculated values are predicting that 3 or 4 helical subunits are involved in the channel structure.

Overall, the conductance values for GBA pores, under our experimental conditions, correspond to the lower conducting states of alamethicin and zervamicin.[12,18,35] The increase in the ionic strength of the solution stabilizes the open pore states. GBA pores show a rectifying behaviour (Fig. 6). The diminishing of conductance at −80 mV, after an instant reversal from +80 mV transbilayer potential, suggests a disruption in the pore structure. This can also account for a general asymmetric orientation in the overall pore structure, as will be discussed later.

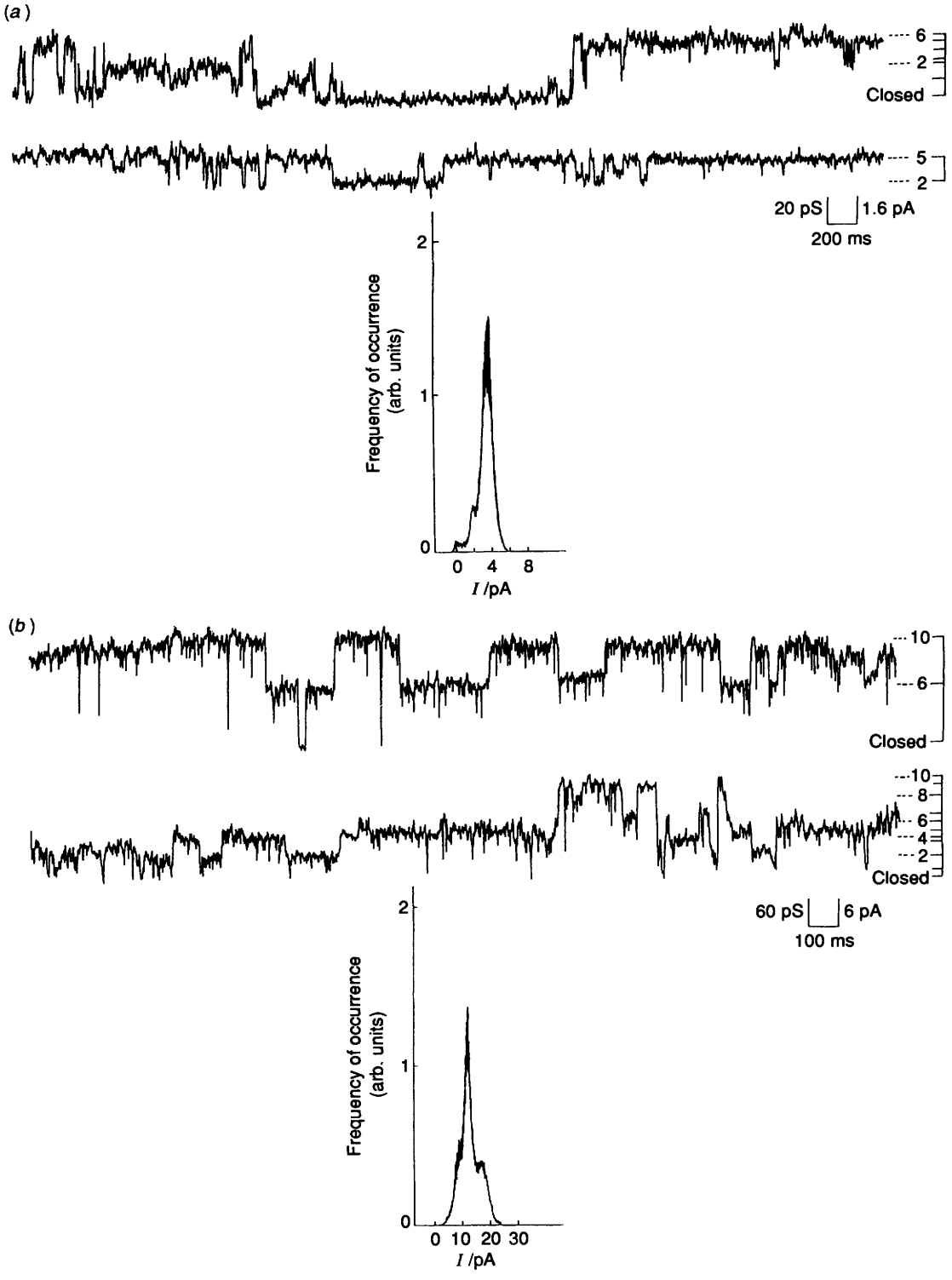


**Fig. 5** Conductance patterns of GBA pores in DPhPC bilayers at a *cis* transbilayer potential of (*a*) +80 mV; and (*b*) +100 mV. The electrolyte solution was composed of 0.5 mol $dm^{-3}$ KCl and buffered with 5 mmol $dm^{-3}$ Hepes at pH 7.4; the electrolyte composition was symmetrical for both sides of the membrane; GBA, at 10 nmol $dm^{-3}$ concentrations, was added to the *cis* side solution, *i.e.* micropipettes; the current amplitude histograms are shown for both (*a*) and (*b*); the scale bars on the right of conductance patterns show conductance states, where the closed state corresponds to the closed pore; the room temperature was 20 ± 1 °C.

**Structure–function relation in GBA**

An α-helical model for GBA (Fig. 7), and the corresponding spatial molecular structure, implies three distinctive parts in the peptide backbone. The *N*-terminus part has a certain structural flexibility due to the presence of Gly at position 2. Then comes a moderately-sized 6-residue sequence from Ala-3 to Aib-8, which suggests a helical motif. From Trp-9 to the end of the sequence bulky amino acid side-chains and Aib appear in an alternative manner. Due to the periodic location of Aib, and the absence of helix-disturbers such as Gly or Pro (common in peptaibol sequences), a generally helical motif from Ala-3 to Trp-15 is plausible for the GBA secondary structure. Another main characteristic of GBA is an asymmetrical overall shape with a bulky *C*-terminus half dominated by aromatic Trp and Phe side-chains, and a comparatively slim *N*-terminus half. Also, in the helical wheel diagram of Fig. 7 the aromatic side-

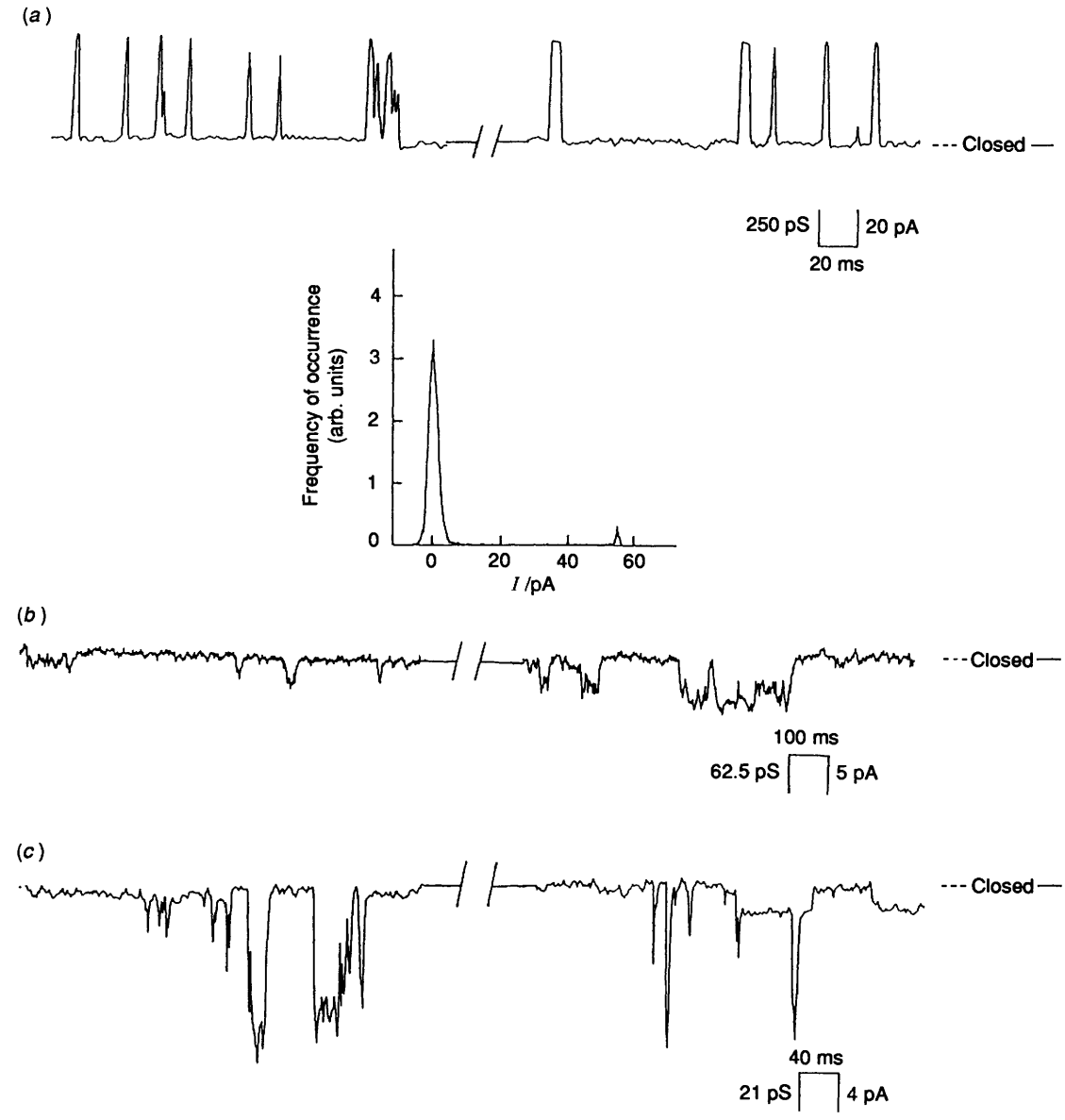


**Fig. 6** Conductance patterns of GBA pores in DPhPC bilayers at a *cis* transbilayer potential of: (*a*) +80 mV (*b*) −80 mV and (*c*) −190 mV. The electrolyte solution was composed of 0.15 mol $dm^{-3}$ KCl, buffered with 5 mmol $dm^{-3}$ Hepes at pH 7.4; the electrolyte composition was symmetrical for both sides of the membrane; GBA at 10 nmol $dm^{-3}$ concentrations was added to the *cis* side solution, *i.e.* micropipettes; the current amplitude histogram is shown for (*a*); the room temperature was 25 ± 1 °C.

**Table 2** Experimental and calculated conductances of GBA in DPhPC bilayers

| Transbilayer potential/mV | KCl concentration/ mol $dm^{-3}$ | Conductance (calculated values)[a]/pS | *N* |
|---|---|---|---|
| +80 | 0.5 | 43.7 (56.8, 43.5) | 3 |
| +100 | 0.5 | 50.0 (56.8, 43.5) | 3 |
| | | 225.0 (380.0, 290.6) | 4 |
| +80 | 0.15 | 137.5 (112.3, 93.2) | 4 |
| | | 268.7 (298.0, 247.4) | 5 |
| | | 687.5 (1008.8, 771.4) | 6 |
| +100 | 0.15 | 20.8 (16.8, 13.9) | 3 |
| | | 16.0 (16.8, 13.9) | 3 |
| +190 | 0.15 | 22.1 (16.8, 13.9) | 3 |
| −190 | 0.15 | 15.8 (16.8, 13.9) | 3 |
| | | 90.0 (112.3, 93.2) | 4 |

[a] Calculated conductances are based on the cylindrical-bundle pore model.[33] The inter-axial distance between two adjacent helices is 1 nm; the helix length for the 16-residue peptide GBA monomer is 2.4 nm; the resistivity ($\rho$) of KCl solutions are either calculated from the limiting ionic conductances at 25 °C (0.13 and 0.44 Ωm for 0.5 and 0.15 mol $dm^{-3}$ KCl solutions, respectively) or experimental values at the same temperature (0.17 and 0.53 Ωm for 0.5 and 0.15 mol $dm^{-3}$ KCl solutions, respectively);[34] the first entry in the parentheses after the experimental conductance corresponds to the calculated values in accordance with the former, and the second entry corresponds to the calculated values in accordance with the latter; '*N*' stands for the number of the helical subunits in the cylindrical-bundle pore.

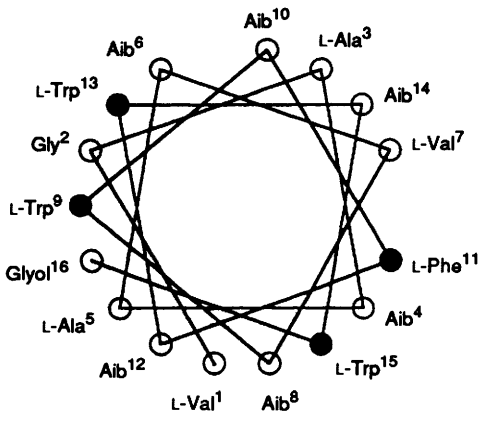


**Fig. 7** Helical wheel diagram of a GBA α-helix

chain orientation have an overall pseudo-plane-symmetry with Trp-9 and Trp-15 on one side, and Phe-11 and Trp-13 on the opposite side.

As revealed in the CD studies, GBA structure is different from both gramicidin and alamethicin (*vide supra*). GBA in water-dominant solvents adopts a different structure from organic solvents. As is observable from the CD spectra (Figs. 2 and 4 and Table 1), the overall helical structure is preserved—though changed in shape—but the maximum–minimum locations are red-shifted and the relative ellipticities indicate a switch to values more than one for the corresponding ratios of $[\theta]_{216}/[\theta]_{209}$ and $[\theta]_{222}/[\theta]_{209}$. This new structure might be caused by an inclusive change in the intra-helical hydrogen-bond pattern and/or an aggregation of this hydrophobic sequence in aqueous solutions. The latter was also suggested for alamethicin in aqueous solutions.[6]

In Fig. 4(*b*), another structural possibility for GBA in vesicles is revealed. Here, in comparison with the spectra in organic solvents, *e.g.* octan-1-ol, the CD spectrum of GBA in EYPC (PL 1:100) shows a decrease in intensity at the maximum around 194 nm, a decrease in negative intensity at 209 nm as well as a red shift in the minimum to 210.4, and an increase in intensity at around 222 nm. The $[\theta]_{222}/[\theta]_{209}$ also changes from 0.90 to 1.07. If we assume a dominantly helical monomeric structure for GBA in octan-1-ol, as is the case with alamethicin,[21] then the spectra in EYPC vesicles will suggest a helix–helix interaction between at least two adjacent helices. In comparison with the helical structures, the same general decrease in the maximum $\pi\pi^*\perp$ positive Cotton effect, and a weakening and red shift in the minimum $\pi\pi^*\parallel$ negative Cotton effect, together with the deepening of the negative Cotton effect at the $n\pi^*$ transition around 222 nm, were also observed in both theoretical,[36] and experimental[5,37] CD structural analysis of coiled-coil tertiary structures.

A basic helical-bundle model can be proposed for the structure of GBA in phospholipid bilayers. This model can also account for the voltage-dependent properties of GBA in a similar manner to alamethicin. The barrel-stave model, as a framework to account for structure-functional properties of alamethicin, has been interpreted in different ways. These interpretations have been reviewed, and preferences are given to certain interpretations such as the stiff helical rod flip-flop model.[3,38] In the majority of these models a certain role has been given to the macrodipoles of α-helical structure of alamethicin in the lipid bilayer interior. A basically similar concept is developed to interpret the pore-forming phenomenon and ion conductance properties of rigid GBA helices in phospholipid bilayers. In this interpretation in addition to the GBA backbone dipole (50.4 D, theoretical estimation),[39] the role of Trp side-chain dipoles (2.08 D)[40] is also considered. At the same time, the relatively high affinity of Trp side-chains for the lipid bilayers, through hydrophobic and electrostatic interactions, has been reported.[41,42] This affinity of the amphiphilic Trp side-chains for the bilayer interfaces might be responsible for relatively low concentrations of GBA used in electrophysiological experiments. Though the peptide concentrations in the channel-detecting experiments were much less than those in CD measurements, it is highly plausible that in both cases the peptide interacts strongly with the membrane and adjacent peptide molecules. The whole event from peptide–lipid interface interactions to channel formation and electrical conductance may be pictured as follows.

GBA helices in aqueous environments, in their monomeric and/or oligomeric states, approach the bilayer surface and are partially adsorbed on the surface (see the CD spectra in water-dominant solvents and phospholipid vesicles). This adsorption is pronounced due to the high affinity of Trp side-chains for membranes, with both hydrophobic and electrostatic interactions. This is possible even in the absence of a transbilayer potential as is suggested by the CD spectra in phospholipid vesicles at low peptide-to-lipid molar ratios. GBA enhances its helical content upon adsorption on the bilayer surface, and possibly partially incorporates in the bilayer hydrophobic interior. Trp residues have this ability to have access to both of the hydrophilic and hydrophobic zones of the lipid bilayer interface and anchor the peptide molecules to the bilayer surface.[41,42] Upon the latter interrelation, a more intense peptide–peptide interaction of the helix–helix type may happen [Fig. 4(*b*)], and this can be especially facilitated in the interior of the bilayer through non-hydrophobic interactions.[43] By applying a *cis*-positive transbilayer potential, an aggregation of pre-formed helical-bundles reorient in parallel to the applied electric field with the *C*-termini (negative end of the helix dipole) of the peptides on the side of the positive potential. An electrostatic inter-dipole repulsion of the parallel dipoles forms a space for the water to enter and the applied potential difference causes the ion transfer through the phospholipid bilayer.[8] Then a dynamic and complex interaction of the helix backbone dipole moment and the dipole moment of Trp side-chains with the applied electric field can cause the observed functional properties of GBA.

In accordance with the rigid cylindrical model, GBA has pore diameters of 0.155 ($N = 3$), 0.414 ($N = 4$), 0.702 ($N = 5$) and 1.00 ($N = 6$) nm. It should be noted that in this model, the effect of the peptide backbone and side-chains on the pore structure, and ion movement through the pore, cannot be considered in detail. The smallest pore should tolerate a drastic conformational change to let $K^+$ (0.266 and 0.66 nm for the respective bare and hydrated ion diameters) or $Cl^-$ (0.362 and 0.66 nm for the respective bare and hydrated ion diameters) pass through. The lowest observed conducting state of alamethicin (with 19 pS conductance for 1 mol $dm^{-3}$ KCl solution),[35] also suggests pores of trimeric conformation. Another possibility is to take higher order structures ($N = 4$ or more) as the simplest conducting structures and assume conformational restrictions for the central pore, as is the case with the membrane protein channel structures such as the proposed pentameric channel model of nAChR.

Finally, in the case of GBA, the presence of the Aib residues results in a rigid stable overall helical structure. Concomitantly, Trp with its respective microdipole, its relative location contiguous to the membrane interface, and its dual amphipathic character, might play an important role in both stabilizing the pore structures of GBA and other small peptides,[40,44,45] and inducing multi-conducting sublevels in the stabilized pores. The incorporation of Aib and Trp in suitable positions in the peptide helical backbone may as well assimilate the effect of the overall tertiary and quaternary structures of proteins in giving

characteristic electrophysiological functions to the corresponding ion channels in membranes.

## Experimental

GBA was synthesized in a previous study.[19] Alamethicin ($R_f$50 fraction as reported previously)[5] and EYPC (100 mg $cm^{-3}$ chloroform solution) were from Sigma (St. Louis, Missouri, USA). DPhPC was obtained from Avanti Polar (Alabaster, Alabama, USA) as 10 mg $cm^{-3}$ chloroform solutions. The solvents used for CD experiments were of extra-pure grade.

CD experiments were performed by a JASCO 720 spectropolarimeter. Quartz cells, in the range of 0.05 to 0.5 cm path lengths, were used for measurements. EYPC unilamellar vesicles were prepared by a probe sonicator in accordance with literature.[46] The peptide was added to appropriate amounts of vesicle aliquots from a 1 mmol $dm^{-3}$ methanolic stock solution. Methanol ratios by volume were 1% in vesicle CD measurements.

Patch-clamp experiments were performed as was generally described,[47] with minor modifications. Patch pipettes were of hard-glass type, and pulled through a two-pull method to give approximate diameters of 1 μm. Pipettes were used without being heat polished or siliconized. Electrolyte solutions were 0.15 or 0.5 mol $dm^{-3}$ KCl solutions buffered with 5 mmol $dm^{-3}$ Hepes [*N*-(2-hydroxyethyl)piperazine-*N'*-2-ethanesulfonic acid] at pH 7.4. The pipette tip resistances in electrolyte solutions were about 10 and 5 MΩ for 0.15 and 0.5 mol $dm^{-3}$ KCl solutions, respectively. Peptide stock solutions were prepared as 1 or 0.5 mmol $dm^{-3}$ ethanolic solutions (stable for several weeks when stored at −20 °C). Peptide final concentrations, when added to patch pipettes, were 10 nmol $dm^{-3}$, and the ratio by volume of ethanol was as low as 0.01%. The chloroform solutions of DPhPC lipids were mildly evaporated, and the residual lipid was redissolved in hexane before being spread on aqueous surfaces. Seals of 2 to 20 GΩ were formed at the tip of pipettes. In some cases a mild suction was applied to increase the seal resistance. Experiments were also performed in the absence of peptide to rule out the possibility of records due to membrane breakdown or non-specific leakage through the formed seals.

Single channel currents were amplified by a CEZ-2300 (Nihon Kohden, Japan) patch/whole cell amplifier, and recorded on a Sony tape-recorder (NFR-3515, Sony, Japan). Data were analysed by a personal computer (PC-98 RL, NEC, Tokyo, Japan), after being transferred from the tape-recorder through a low-pass filter (E-3201 A, NF, Tokyo, Japan) with a 500 Hz cut-off frequency.

## Acknowledgements

We wish to express our thanks to Mr. Hiroki Takahashi for his active and worthwhile contribution to this work. We also appreciate the kind technical assistance of Dr. Hiroshi Matsuura and Dr. Takao Shioya of Saga Medical School.

This work was supported in part by research grants from the Ministry of Education, Science and Culture of Japan (05453206).

## References

1 N. Unwin, *Neuron*, 1989, **3**, 665.
2 B. A. Wallace, *Annu. Rev. Biophys. Biophys. Chem.*, 1990, **19**, 127.
3 G. A. Woolley and B. A. Wallace, *J. Membrane Biol.*, 1992, **129**, 109.
4 H. Vogel, *Biochemistry*, 1987, **26**, 4562.
5 G. A. Woolley and B. A. Wallace, *Biochemistry*, 1993, **32**, 9819.
6 G. Jung, N. Dubischar and D. Leibfritz, *Eur. J. Biochem.*, 1975, **54**, 395.
7 R. O. Fox, Jr. and F. M. Richards, *Nature (London)*, 1982, **300**, 325.
8 G. Boheim, W. Hanke and G. Jung, *Biophys. Struct. Mech.*, 1983, **9**, 181.
9 A. W. Burgess and S. J. Leach, *Biopolymers*, 1973, **12**, 2599.
10 I. L. Karle and P. Balaram, *Biochemistry*, 1990, **29**, 6747.
11 G. R. Marshall, E. E. Hodgkin, D. A. Langs, G. D. Smith, J. Zabrocki and M. T. Leplawy, *Proc. Natl. Acad. Sci. USA*, 1990, **87**, 487.
12 M. S. P. Sansom, *Prog. Biophys. Mol. Biol.*, 1991, **55**, 139.
13 M. S. P. Sansom, *Eur. Biophys. J.*, 1993, **22**, 105.
14 D. J. Barlow and J. M. Thornton, *J. Mol. Biol.*, 1988, **201**, 601.
15 J.-P. Changeux, A. Devillers-Thiéry and P. Chemouilli, *Science*, 1984, **225**, 1335.
16 G. Menestrina, K.-P. Voges, G. Jung and G. Boheim, *J. Membrane Biol.*, 1986, **93**, 111.
17 R. Latorre and O. Alvarez, *Physiol. Rev.*, 1981, **61**, 77.
18 P. Balaram, K. Krishna, M. Sukumar, I. R. Mellor and M. S. P. Sansom, *Eur. Biophys. J.*, **21**, 117.
19 M. Jelokhani-Niaraki, K. Yoshioka, H. Takahashi, F. Kato and M. Kondo, *J. Chem. Soc., Perkin Trans. 2*, 1992, 1187.
20 M. Kondo, H. Takahashi, M. Jelokhani-Niaraki, T. Ehara, T. Shioya and H. Kodama, in *Peptide Chemistry 1993*, ed. Y. Okada, Protein Research Foundation, Osaka, 1994, p. 437.
21 R. Yantarno, S. Takashima and P. Mueller, *Biophys. J.*, 1982, **38**, 105.
22 G. Schwarz and P. Savko, *Biophys. J.*, 1982, **39**, 211.
23 D. W. Urry, J. D. Glickson, D. F. Mayers and J. Haider, *Biochemistry*, 1972, **11**, 487.
24 K.-L. Voges, G. Jung and W. H. Sawyer, *Biochim. Biophys. Acta*, 1987, **896**, 64.
25 K. Otoda, S. Kimura and Y. Imanishi, *Biochim. Biophys. Acta*, 1993, **1150**, 1.
26 A. Iida, S. Uesato, T. Shingu, Y. Nagaoka, Y. Kuroda and T. Fujita, *J. Chem. Soc., Perkin Trans. 1*, 1993, 375.
27 B. A. Wallace, W. R. Veatch and E. R. Blout, *Biochemistry*, 1981, **20**, 5754.
28 G. E. Arnold, L. A. Day and A. K. Dunker, *Biochemistry*, 1992, **31**, 7948.
29 P. Mueller and D. O. Rudin, *Nature (London)*, 1968, **217**, 713.
30 B. Sakmann and G. Boheim, *Nature (London)*, 1979, **282**, 336.
31 M. Eisenberg, J. E. Hall and C. A. Mead, *J. Membrane Biol.*, 1973, **14**, 143.
32 J. E. Hall, I. Vodyanoy, T. M. Balasubramanian and G. R. Marshall, *Biophys. J.*, 1984, **45**, 233.
33 B. Hille, *Ionic Channels of Excitable Membranes*, Sinauer Associates, Massachusetts, 1992, 2nd edn.
34 R. A. Robinson and R. H. Stokes, in *Electrolyte Solutions*, Butterworths, London, 1970, 2nd edn.
35 W. Hanke and G. Boheim, *Biochim. Biophys. Acta*, 1980, **596**, 456.
36 T. M. Cooper and R. W. Woody, *Biopolymers*, 1990, **30**, 657.
37 N. E. Zhou, B.-Y. Zhu, C. M. Kay and R. S. Hodges, *Biopolymers*, 1992, **32**, 419.
38 L. P. Kelsh, J. F. Ellena and D. S. Cafiso, *Biochemistry*, 1992, **31**, 5136.
39 W. G. Hol, *Adv. Biophys.*, 1985, **19**, 133.
40 W. Hu, K.-C. Lee and T. A. Cross, *Biochemistry*, 1993, **32**, 7035.
41 R. E. Jacobs and S. H. White, *Biochemistry*, 1989, **28**, 3421.
42 W. C. Wimley and S. H. White, *Biochemistry*, 1993, **32**, 6307.
43 J.-L. Popot and D. M. Engelman, *Biochemistry*, 1990, **29**, 4031.
44 J. Deisenhofer and H. Michel, *EMBO J.*, 1989, **8**, 2149.
45 A. Kreusch, A. Neubüser, E. Schiltz, J. Weckesser and G. E. Schultz, *Protein Sci.*, 1994, **3**, 58.
46 R. R. C. New, in *Liposomes, A Practical Approach*, ed. R. R. C. New, IRL Press, Oxford, 1990, p. 33.
47 R. Coronado and R. Latorre, *Biophys. J.*, 1983, **43**, 231.

*Paper* 4/05535G
*Received* 12*th September* 1994
*Accepted* 15*th November* 1994